Eddy Energy Fluxes in Mixed Barotropic–Baroclinic Instability: Upgradient or Downgradient?

Madeleine K. Youngs

October 21, 2019

1 Introduction

Wave-type instabilities, such as barotropic and baroclinic instability, are important types of variability in the oceanic and atmospheric system. These instabilities generate storms in the atmosphere and eddies in the ocean, set the stratification of the global ocean [*Marshall and Speer*, 2012], generate surface westerlies in the atmosphere (see *Vallis* [2006] and references therein) and more. They are generally important for setting the mean state of the system. In the ocean, these instabilities are parameterized as a diffusion of buoyancy along isopycnals, which decreases the baroclinic shear, but does nothing to account for barotropic instability or the momentum fluxes associated with both instabilities and their effects on the mean flow, because they are too complicated [*Gent and McWilliams*, 1990]. In effect, the mean state of ocean models is likely to be inaccurate at best in some regions. I examine these momentum fluxes to determine the effects of eddies on the mean flow.

The necessary conditions for barotropic and baroclinic instability state that there must be a sign change of the potential vorticity (PV) gradient somewhere in the domain for instability to occur [*Charney and Stern*, 1962]. Purely barotropic flow and thus instability would have a sign change of the PV gradient within a layer, which would indicate a downgradient momentum flux and extraction of energy from the mean flow [*Rayleigh*, 1880; *Drazin and Howard*, 1966]. For a purely baroclinic flow, there must be a sign change in the PV gradient between the layers and this results in a downgradient flux of buoyancy and extraction of energy from available potential energy [*Eady*, 1949; *Charney*, 1947]. In the real world, however, flows have both vertical and horizontal shear and thus have two mean energy reservoirs, kinetic and potential energy. The necessary conditions for instability in this case don't indicate which energy reserves are being tapped, but just that energy is being extracted from the mean. Thus, it would be useful to be able to determine a priori the energy pathways in an unstable system, but so far this goal has been elusive. For example, it is sometimes assumed that a change in sign of the PV gradient in a layer implies that there is a down-gradient momentum flux [*Pedlosky*, 1964]. This assumption is false. I show that the dynamical interaction between layers is responsible for setting the direction of the momentum fluxes in a linearly unstable system.

In a baroclinically unstable fluid with a horizontal shear, interesting interactions occur between the instability and the horizontal shear. There can be upgradient momentum fluxes associated with the baroclinic instability [*Pedlosky*, 1964], but also downgradient momentum fluxes. *Held* [1975] found that when a two-layer flow has the same sign PV gradient in both layers, the direction of the momentum fluxes can be determined. *Killworth* [1980] examines the parameter space of instabilities with horizontal and vertical shear and found that when the horizontal length scale of the shear was larger than the internal deformation radius, then baroclinic conversion dominated, but when the

horizontal length scale was much smaller than the deformation radius, then barotropic conversion dominated (see also *Holland and Haidvogel* [1980]).

In this report I look at the linear stability of a zonal channel flow to understand the direction of the momentum and buoyancy fluxes of a wide parameter space and answer the question: what sets the direction of the eddy energy fluxes in mixed instability? In section 2, I set up the model and diagnostics used to analyze the momentum fluxes. In sections 3 and 4, I describe the Gaussian and cosine jet configurations, respectively. I conclude in section 5.

2 Model

2.1 Linear stability problem

The derivation that follows parallels *Pedlosky* [1987]. I consider the two–layer quasi–geostrophic potential vorticity (QGPV) non-dimensionalized equations on a β-plane:

$$\left[\frac{\partial}{\partial t} + \frac{\partial \psi_n}{\partial x}\frac{\partial}{\partial y} - \frac{\partial \psi_n}{\partial y}\frac{\partial}{\partial x}\right]\left[\beta y + \nabla^2\psi_n - F_n(-1)^n(\psi_2 - \psi_1) + \eta_b\delta_{n2}\right] = 0 \qquad n = 1, 2 \tag{1}$$

where ψ_n is the stream function, δ_{ij} is the Kronecker delta function and

$$\nabla^2 = \frac{\partial^2}{\partial x^2} + \frac{\partial^2}{\partial y^2}.$$

I have

$$\beta = \beta_0 \frac{L^2}{U} \tag{2}$$

where β_0 is the meridional gradient in planetary vorticity, L is a length scale given by the width of the channel, and U is the velocity scale of the jet and

$$F_n = \frac{f_0^2 L^2}{g(\rho_2 - \rho_1)/\rho_0 D_n} \tag{3}$$

where f_0 is the planetary vorticity, ρ_n is the density of the n-th layer, ρ_0 is a reference density and D_n is the depth of the layer and

$$F = \frac{f_0^2 L^2}{g(\rho_2 - \rho_1)/\rho_0 D} \tag{4}$$

where D is the total depth. I relate F_n to F by a ratio of depth of top layer to lower layer $\Delta = D_1/D_2$: $F_1 = F(1+\Delta)/\Delta$ and $F_2 = F(1+\Delta)$. The topographic forcing is given by:

$$\eta_b = \frac{f_0 h_b}{D_2}\frac{L}{U} \tag{5}$$

and is only included in the lowest layer.

I consider a zonal basic flow

$$U_n(y) = -\frac{\partial \Psi_n}{\partial y} \tag{6}$$

that has a horizontal shear as a source of kinetic energy and a vertical shear (through thermal wind) as a source of available potential energy. Let ϕ_n be the eddy stream function such that

$$\psi_n = \Psi_n(y) + \phi_n(x, y, t) \tag{7}$$

with eddy velocities

$$u_n = -\frac{\partial \phi_n}{\partial y}, \qquad v_n = \frac{\partial \phi_n}{\partial x} \tag{8}$$

I substitute Eq. 7 into Eq. 1 to get:

$$\left[\frac{\partial}{\partial t} + U_n \frac{\partial}{\partial x}\right] q_n + \frac{\partial \phi_n}{\partial x}\frac{\partial Q_n}{\partial y} + \left[\frac{\partial \phi_n}{\partial x}\frac{\partial q_n}{\partial y} - \frac{\partial \phi_n}{\partial y}\frac{\partial q_n}{\partial x}\right] = 0 \tag{9}$$

where the potential vorticity gradient of the basic state is

$$\frac{\partial Q_n}{\partial y} = \beta - \frac{\partial^2 U_n}{\partial y^2} - F_n(-1)^n(U_1 - U_2) + \frac{\partial \eta_b}{\partial y}\delta_{n2} \tag{10}$$

and the perturbation potential vorticity is given by

$$q_n = \nabla^2 \phi_n - F_n(-1)^n(\phi_2 - \phi_1) \tag{11}$$

We then consider the linear stability problem by neglecting the terms of order $\mathcal{O}(\phi_n^2)$ and higher where I get the linearized QGPV equation.

$$\left[\frac{\partial}{\partial t} + U_n \frac{\partial}{\partial x}\right] q_n + \frac{\partial \phi_n}{\partial x}\frac{\partial Q_n}{\partial y} = 0 \tag{12}$$

with boundary conditions

$$\frac{\partial \phi_n}{\partial x} = 0, \qquad y = \pm 1 \tag{13}$$

which says that there is no flow into or out of the walls at the boundary.

The necessary conditions for instability in this case are given by:

$$\int_{-1}^{1} dy \sum_n \frac{\partial}{\partial t}\frac{|\phi_n|^2}{|U_n - c|^2}\frac{\partial Q_n}{\partial y} = 0 \tag{14}$$

where c is the phase speed of the wave as developed in section 2.2. This equation is derived from the zonally averaged momentum equation. If the flow is unstable, $\frac{\partial}{\partial t}\frac{|\phi_n|^2}{|U_n - c|^2}$ must be positive such that the eddy energy is growing, so in order for this equation to be satisfied, $\frac{\partial Q_n}{\partial y}$ must change sign somewhere in the domain.

2.2 Diagnostics

In order to understand the energetics of the flow, I use the energy equation for the perturbations. I set $D_n/D = d_n$. I take Eq. 12 and multiply by $-d_n\phi_n$ and sum the two layers, and integrate in y.

$$\frac{\partial}{\partial t}\int_{-1}^{1} dy\,[\mathrm{EKE}_1 + \mathrm{EKE}_2 + \mathrm{EAPE}] = \int_{-1}^{1} dy\,[\Delta\mathrm{EKE}_1 + \Delta\mathrm{EKE}_2 + \Delta\mathrm{EAPE}] \tag{15}$$

$$\mathrm{EKE}_n = \frac{d_n}{2}\overline{\left(\frac{\partial \phi_n}{\partial x}\right)^2 + \left(\frac{\partial \phi_n}{\partial y}\right)^2} \tag{16}$$

$$\mathrm{EAPE} = \frac{\overline{(\phi_1 - \phi_2)^2}}{2}F_0 \tag{17}$$

$$\Delta\mathrm{EKE}_n = d_n\overline{\frac{\partial \phi_n}{\partial x}\frac{\partial \phi_n}{\partial y}}\frac{\partial U_n}{\partial y} \tag{18}$$

$$\Delta\mathrm{EAPE} = F_0(U_1 - U_2)\overline{\frac{\partial \phi_2}{\partial x}\phi_1} \tag{19}$$

where the left-hand side represents the time change of total eddy energy and the right-hand side represents the conversion from the mean into the eddy energy. If there is energy converted into eddies through a positive (negative) ΔEKE_n, then the momentum fluxes are said to be downgradient (upgradient) because they act to relax (strengthen) the mean flow and transfer kinetic energy from regions of high (low) energy to regions of low (high) kinetic energy. If there is energy converted into eddies through a positive (negative) ΔEAPE, then the buoyancy fluxes are said to be downgradient (upgradient) because they act to relax (strengthen) the mean buoyancy gradient and transfer potential energy from regions of high (low) potential energy to regions of low (high) potential energy.

Another way to assess how eddies affect the mean flow is to consider the zonally averaged, zonal momentum equation summed over both layers:

$$\frac{\partial}{\partial t}\left[\sum_{n=1}^{2} d_n \overline{u_n}\right] = -\frac{\partial}{\partial y}\left[\sum_{n=1}^{2} d_n \overline{u_n v_n}\right] \tag{20}$$

so the change of zonal momentum is related to the divergence of the Reynolds stresses. I can take the PV equation and the enstrophy equation to show that

$$\frac{\partial}{\partial t}\left[\sum_{n=1}^{2} d_n \overline{u_n}\right] = -\frac{\partial}{\partial y}\left[\sum_{n=1}^{2} d_n \frac{\overline{q_n^2}}{\partial Q_n/\partial y}\right] \tag{21}$$

Ultimately, I want to know if the barotropic flow accelerates or decelerates, and this expression tells us that I know the sign of the acceleration if $\partial Q_n/\partial y$ has the same sign in both layers [*Held*, 1975]. If the PV gradients are not the same sign then the sign of the acceleration also depends on the ratio of the magnitudes of $\overline{q_n^2}$ as well as $\partial Q_n/\partial y$.

2.3 Eigenvalue solver

I use an eigenvalue solver to compute the solutions to Eq. 12. First I assume a solution of the form

$$\phi_n = \text{Re } \Phi_n(y) e^{ik(x-ct)} \tag{22}$$

where Eq. 12 becomes two coupled ordinary differential equations

$$(U_1 - c)\left[\frac{d^2\Phi_1}{dy^2} - k^2\Phi_1 - F_1(\Phi_1 - \Phi_2)\right] + \Phi_1 \frac{\partial Q_1}{\partial y} = 0 \tag{23}$$

$$(U_2 - c)\left[\frac{d^2\Phi_2}{dy^2} - k^2\Phi_2 - F_2(\Phi_2 - \Phi_1)\right] + \Phi_2 \frac{\partial Q_2}{\partial y} = 0 \tag{24}$$

I discretize the various parameters across my channel and use second order finite differencing to create a differentiation matrix for the operator $\frac{d^2}{dy^2}$ which gives an equivalent matrix expression for Equations 23 and 24. Then for every k, I can use an eigenvalue solver to compute the eigenvalues c and the eigenvectors $\left[\frac{d^2\Phi_n}{dy^2} - k^2\Phi_n + F_n(-1)^n(\Phi_1 - \Phi_2)\right]$ and Φ_n. Then I normalize Φ_n so that the total energy in the domain is 1 ($\text{EKE}_1 + \text{EKE}_2 + \text{EAPE} = 1$). Then growth rates kc_i and energy conversions are computed (Eq. 18 and 19). After computing the solution for all ks the solution (Φ_n) with maximum growth rate (kc_i) is selected for further analysis. In reality, the solution that is selected is not always the one with the maximum growth rate but can be another mode [*Pedlosky*, 1981].

3 Gaussian Jet

3.1 Set up

I set up the two layers with a Gaussian jet of half-width δ in the upper layer and no flow in the lower layer (Fig. 1).

$$U_1 = \frac{1}{2} + \frac{1}{2}e^{-\frac{y^2}{\delta^2}} \tag{25}$$

$$U_2 = 0 \tag{26}$$

Note that the velocity has been scaled out of the problem and is included in the β parameter. δ ranges from 0 to 1 in our non-dimensionalized domain. In this case the basic state potential vorticity gradient is given by

$$\frac{\partial Q_1}{\partial y} = \beta - \frac{\partial^2 U_1}{\partial y^2} + F_1 U_1 \tag{27}$$

$$\frac{\partial Q_2}{\partial y} = \beta - F_2 U_1 \tag{28}$$

We have 4 non-dimensional parameters to vary in this case: F_0, δ, Δ, and β. For experiments discussed here, I set $\Delta = 1$.

3.2 Results

I examine the energy conversion over a range of F and β and set $\delta = 0.05$ as a constant. I scale the constants F and β with δ^2. This rescales the

$$F\delta^2 = F = \frac{f_0^2 \delta_0^2}{g(\rho_2 - \rho_1)/\rho_0 D} \tag{29}$$

and

$$\beta\delta^2 = \beta_0 \frac{\delta_0^2}{U} \tag{30}$$

where $\delta = \delta_0/L$ is the length scale of the jet width. First, I notice that when the PV gradient changes sign in the upper layer, the momentum fluxes are not always downgradient (Fig. 2). There are also downgradient momentum fluxes associated with no sign change of the PV gradient in the upper layer. So, it is not the introduction of a sign change in the upper-layer PV gradient that leads to downgradient momentum fluxes. I also notice that as I decrease F or increase the deformation radius, the kinetic energy conversion comes to dominate over the potential energy conversion.

I split up the domain into 5 regions. Region 1 has downgradient momentum fluxes but no sign change in the upper layer PV gradient; this is an unexpected result. Region 2 has downgradient momentum fluxes and a sign change in the upper layer PV gradient. Region 3 has upgradient momentum fluxes and no sign change in the upper layer PV gradient. Region 4 has upgradient momentum fluxes and a sign change in the upper layer PV gradient; this is also an unexpected result. Region 5 is dominated by barotropic conversion and has a sign change in the upper layer PV gradient.

In these 5 different regions, there are defining characteristics in the wavenumber space (Fig. 3). In regions 1-4, the dominant mode (with largest growth rate) is a mode with primarily baroclinic production (downgradient buoyancy fluxes) and weak barotropic production (kinetic energy fluxes).

When a mode has primarily kinetic energy conversion, I call it a barotropic mode and when it has primarily baroclinic conversion, I call it a baroclinic mode. Regions 1 and 2 have downgradient kinetic energy fluxes and regions 3 and 4 have upgradient kinetic energy fluxes at the most unstable wavenumber. Comparing region 1 and region 2, the primary difference is that modes with higher wavenumber appear. These new modes have primarily barotropic conversion. Similarly, this mode appears in region 4 but not region 3. So when the sign change is introduced into the upper layer PV gradient in regions 2 and 4, a higher-wavenumber barotropic mode appears as a solution. In these regions, the dominate barotropic modes both have locations where $U_1 - c$ vanishes. This indicates that the barotropic modes are contiguous with neutral modes, and is a result consistent with previous studies [*Kuo*, 1949]. The dominant (baroclinic) mode sets the direction of the momentum fluxes in regions 1-4 and the mode primarily dependent on F, β, and δ and not on the upper-layer PV gradient in particular. In region 5, the baroclinic mode's growth rate decreases but the barotropic mode's growth rate increases and becomes dominant.

The direction of the momentum fluxes in the baroclinic mode can be visualized geometrically (Fig. 4). When the stream function is tilted with the flow, then the fluxes are upgradient and energy is being fed back into the mean, but when the stream function is tilted against the flow, then the momentum fluxes are downgradient and energy is being extracted from the mean. In region 2 near the center of the jet, the stream function is tilted against the flow, leading to downgradient momentum fluxes. In region 3 near the center of the jet, the stream function is tilted with the flow, indicating upgradient momentum fluxes. This shows us that the particular arrangement of the stream function in the baroclinic mode is important for setting the direction of the momentum fluxes.

As I increase δ similar structures appear but the line that separates upgradient and downgradient momentum fluxes moves to the right (larger $\beta\delta^2$), eventually until there is no region 4 (Fig. 5). This indicates the role of the channel walls in setting the structure of the streamfunction and the direction of the fluxes.

3.3 Physical interpretation

As I reduce F, I reduce the coupling between the layers or increase the internal deformation radius. Physically this corresponds to a weakening of the baroclinic mode, largely without modifying the barotropic mode. The deformation radius becomes much larger than the length scale defining the horizontal shear ($F\delta^2 << 1$), making PV gradients and growth rates dominated by the horizontal shear. When $F\delta^2 >> 1$ the baroclinic mode dominates. This result is discussed at length in *Killworth* [1980].

4 Cosine Jet

In the previous section, I examined the cases where there was always a sign change between the two layers, which doesn't allow an examination of cases with no sign change between two layers. By examining set-ups where there is no change in the PV gradient between layers but a change within each layer, I examine cases that are analogous to the Gaussian jet set-up where there is no change in the PV gradient within the layer. By comparing these two cases, I expect a super-symmetry in this system because baroclinic and barotropic instability are described by the same eigenvalue problem [*Drazin and Reid*, 2004] and a just a rotation of the same system.

4.1 Set up

I set up a cosine jet in this case, so that I can set up a flow where the potential vorticity gradient can be the same sign between the two layers but a different sign within the layer (Fig. 6). I introduce topography into my lower layer in order to force the PV gradients to change sign at the same location. My flow is then:

$$U_1 = 1/2 + 1/2\cos(\pi y) \tag{31}$$

$$U_2 = 0 \tag{32}$$

The topography that I construct is

$$\frac{\partial \eta_b}{\partial y} = \gamma \cos(\pi y) + C \tag{33}$$

The potential vorticity gradient

$$\frac{\partial Q_1}{\partial y} = \beta + \frac{\pi^2}{2}\cos(\pi y) + \frac{F_1}{2}(1 + \cos(\pi y)) \tag{34}$$

$$\frac{\partial Q_2}{\partial y} = \beta - \frac{F_2}{2}(1 + \cos(\pi y)) + \gamma \cos(\pi y) + C \tag{35}$$

where $\gamma = 8$ is the magnitude of the topography variation and C is the magnitude of the constant slope added to enforce the condition that the PV gradient change sign at the same location in both layers.

4.2 Results

I analyze this configuration following section 3 by varying F and β and interpreting the eddy energy conversion. There are three distinct regions in the domain (Fig. 7). Region 1 has upgradient buoyancy fluxes and downgradient momentum fluxes and has no sign change between the two layers. Region 2 has downgradient buoyancy fluxes and downgradient momentum fluxes and has no sign change between the two layers (this is counter intuitive). Region 3 has downgradient buoyancy fluxes and has a sign change between the two layers. Notice that unlike the Gaussian jet case, there is no region with upgradient buoyancy fluxes but a sign change between the layers.

In comparing region 1 and region 2, the buoyancy fluxes change from upgradient to downgradient (Fig. 8). This is seen in the barotropic mode of the flow. As the sign change between the two layers is introduced a baroclinic mode is introduced, just as I found in section 3.2 for the barotropic mode. I see a symmetry in the modes that appear.

4.3 Physical Interpretation

As I increase F, I increase the coupling between the two layers so the baroclinic mode becomes stronger and eventually dominates. With a smaller β I see a larger region of down-gradient buoyancy fluxes but no sign change. In the Gaussian jet case the walls act to eliminate region 4, or the region with upgradient momentum fluxes with a sign change in the upper layer PV gradient, but in this case there is no region with upgradient buoyancy fluxes with a sign change between the layers. The QG approximation involves assuming that the layers are thin, which seems to be preventing a region with upgradient buoyancy fluxes and a sign change between the layers, just like the walls prevent region 4 in the Gaussian jet.

5 Conclusion

In this report, I have shown that the change in sign of the PV gradient within a layer (between layers) is not generally responsible for setting the sign of the eddy momentum (buoyancy) fluxes. I have shown that the relative magnitude of the eddy PV of the two layers is fundamental for determining the direction of the eddy momentum fluxes. The relative magnitude of the eddy PV is set by the PV gradients, the position of the walls, and the structure of the most unstable mode, but there is not a straightforward way to determine the relative magnitude.

References

Charney, J. G. *The Dynamics of Long Waves in a Baroclinic Westerly Current*, doi:10.1175/1520-0469(1947)004<0136:TDOLWI>2.0.CO;2, 1947.

Charney, J. G., and M. E. Stern. *On the Stability of Internal Baroclinic Jets in a Rotating Atmosphere*, Journal of the Atmospheric Sciences, *19*(2), 159–172, doi:10.1175/1520-0469(1962)019<0159:OTSOIB>2.0.CO;2, 1962.

Drazin, P. G., and L. N. Howard, Hydrodynamic Stability of Parallel Flow of Inviscid Fluid, *Advances in Applied Mechanics*, *9*(C), 1–89, doi:10.1016/S0065-2156(08)70006-1, 1966.

Drazin, P. G., and W. H. Reid, Hydrodynamic Stability, *Cambridge University Press*, p. 605, doi:10.1017/CBO9780511616938, 2004.

Eady, E. T., Long Waves and Cyclone Waves, *Tellus*, *1*(3), 33–52, doi:10.3402/tellusa.v1i3.8507, 1949.

Gent, P. R., and J. C. McWilliams, Isopycnal Mixing in Ocean Circulation Models, *Journal of Physical Oceanography*, *20*(1), 150–155, doi:10.1175/1520-0485(1990)020<0150:IMIOCM>2.0.CO;2, 1990.

Held, I. M., Momentum Transport by Quasi-Geostrophic Eddies, *Journal of the Atmospheric Sciences,* doi:10.1175/15200469(1975)032<1494:MTBQGE>2.0.CO;2, 1975.

Holland, W. R., and D. B. Haidvogel, A Parameter Study of the Mixed Instability of Idealized Ocean Currents, *Dynamics of Atmospheres and Oceans*, *4*(3), 185–215, doi:10.1016/0377-0265(80)90014-7, 1980.

Killworth, P. D., Barotropic and Baroclinic Instability in Rotating Stratified Fluids, *Dynamics of Atmospheres and Oceans*, *4*(3), 143–184, doi:10.1016/0377-0265(80)90013-5, 1980.

Kuo, H.-l., Dynamic Instability of Two-dimensional Nondivergent Flow in a Barotropic Atmosphere, *Journal of Meteorology*, *6*(2), 105–122, doi:10.1175/ 1520-0469(1949)006<0105:DIOTDN>2.0. CO;2, 1949.

Marshall, J., and K. Speer, Closure of the Meridional Overturning Circulation through Southern Ocean Upwelling, *Nature Geoscience*, *5*(3), 171–180, doi:10.1038/ngeo1391, 2012.

Pedlosky, J., The Stability of Currents in the Atmosphere and the Ocean: Part II, *Journal of the Atmospheric Sciences,* doi:10.1175/1520-0469(1964)021<0342:TSOCIT>2.0.CO;2, 1964.

Pedlosky, J., The nonlinear dynamics of baroclinic wave ensembles, *J. Fluid Mech.*, *102*(-1), 169–209, doi:10.1017/S0022112081002590, 1981.

Pedlosky, J., Geophysical Fluid Dynamics, *New York and Berlin, Springer-Verlag, 1982. 636 . . .*, p. 742, doi:10.1007/978-1-4612-4650-3, 1987.

Rayleigh, L., On the Stability, or Instability, of Certain Fluids Motions II., *Proceedings of the London Mathematical Society*, *1*(1), 57–72, doi:10.1112/plms/s1-11.1.57, 1880.

Vallis, G. K., Atmospheric and Oceanic Fluid Dynamics, *Cambridge University Press*, p. 773, doi:10.1002/qj.186, 2006.

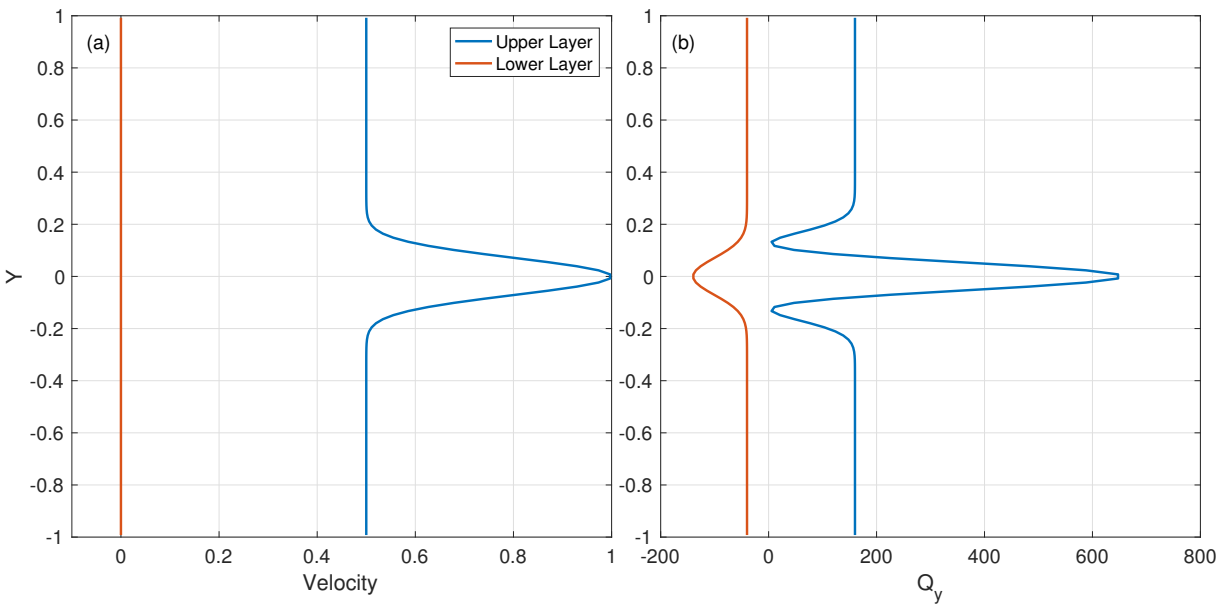

Figure 1: An example velocity profile and PV gradient for $\beta = 60$, $F = 100$ and $\delta = 0.1$.

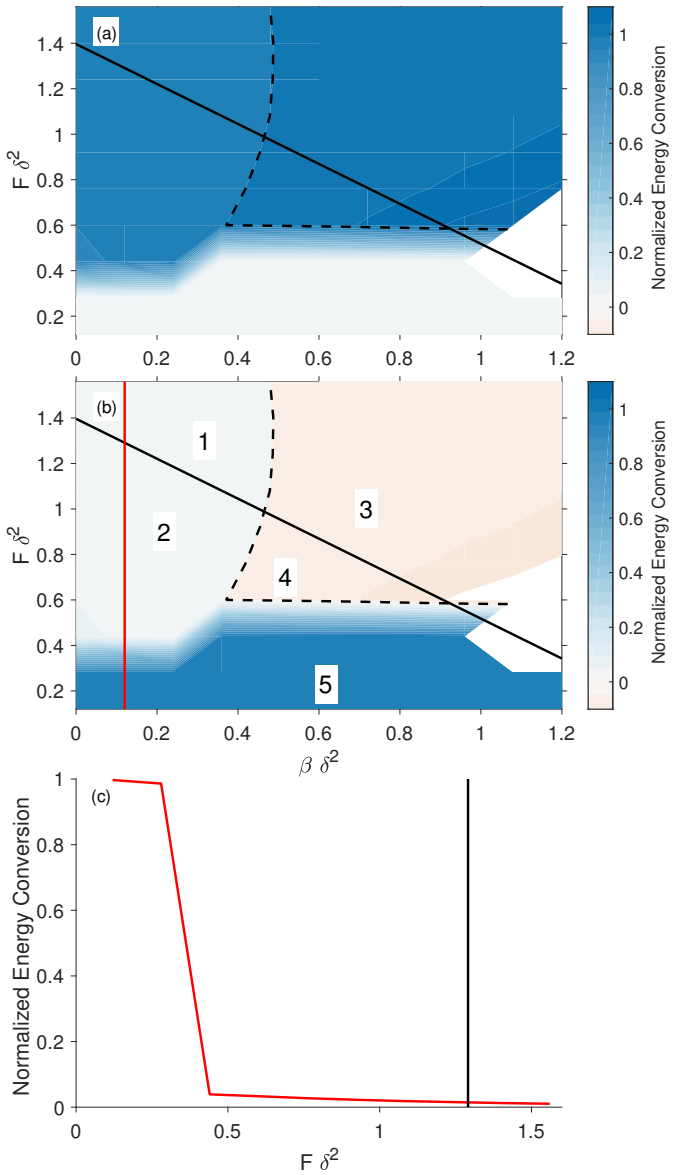

Figure 2: Energy conversion computed for the most unstable eigenfunctions normalized by total (potential plus kinetic) energy conversion at $\delta = 0.05$. Potential energy conversion (a) and kinetic energy conversion (b). The domain is divided into 5 regions. The dotted line shows where the momentum fluxes change sign and the solid line shows where the upper layer PV gradient changes sign, with no sign change to the right and a sign change to the left. Blue represents downgradient fluxes and red represents upgradient fluxes. A cross section of kinetic energy conversion (c) as shown in red line of panel (b).

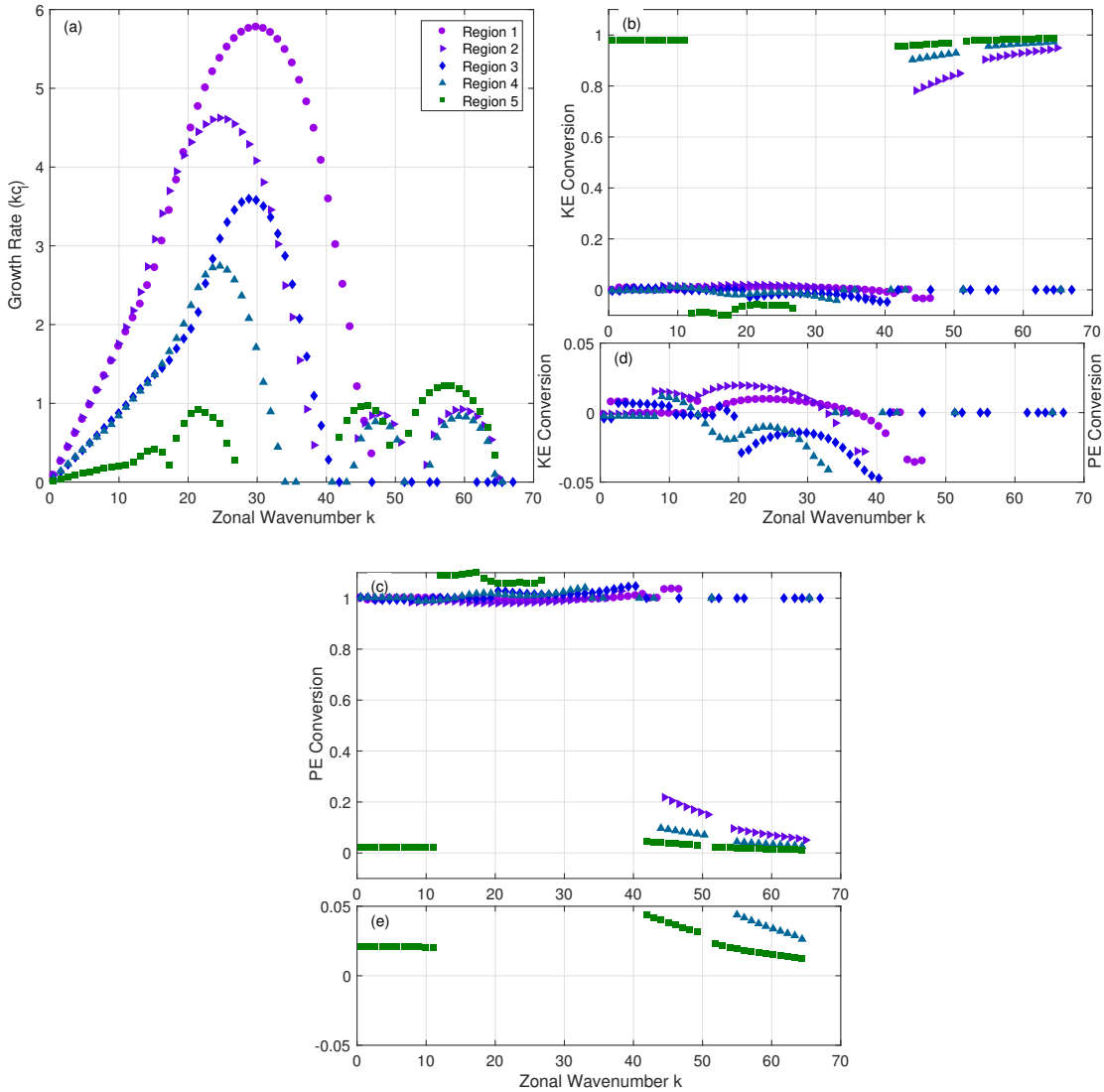

Figure 3: Example growth rates and normalized energy conversions from 5 different regions. Growth rates (a), kinetic energy conversion (b,d) and potential energy conversion (c,e). Region 1: $\beta = 120$, $\delta = 0.05$, $F = 520$. Region 2: $\beta = 80$, $\delta = 0.05$, $F = 360$. Region 3: $\beta = 280$, $\delta = 0.05$, $F = 400$. Region 4: $\beta = 200$, $\delta = 0.05$, $F = 280$. Region 5: $\beta = 240$, $\delta = 0.05$, $F = 200$.

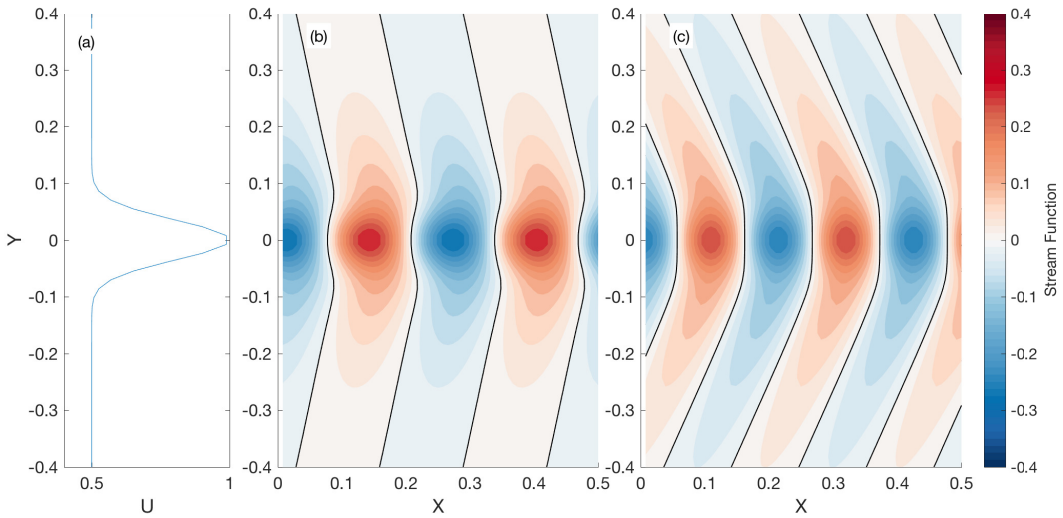

Figure 4: A jet profile (a) with the most unstable eigenfunction plotted in space given at $\beta = 20$, $\delta = 0.05$ and $F = 360$ in region 2 (b) and at $\beta = 320$, $\delta = 0.05$ and $F = 400$ in region 3 (c).

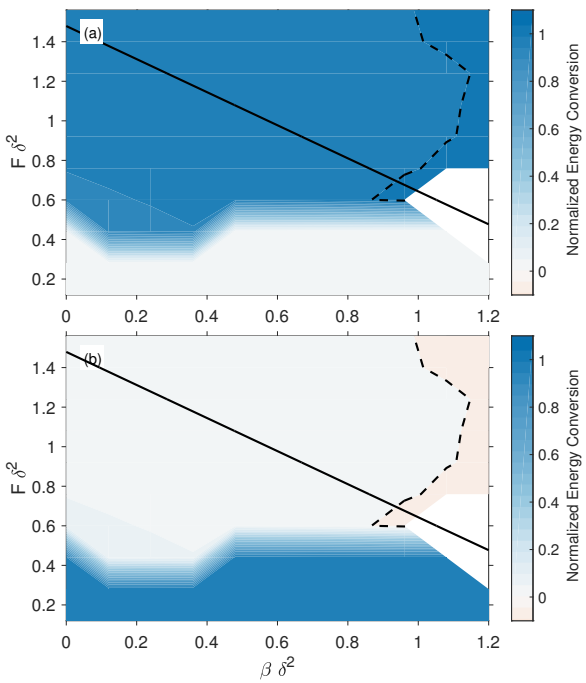

Figure 5: Same as Fig. 2 but for $\delta = 0.3$.

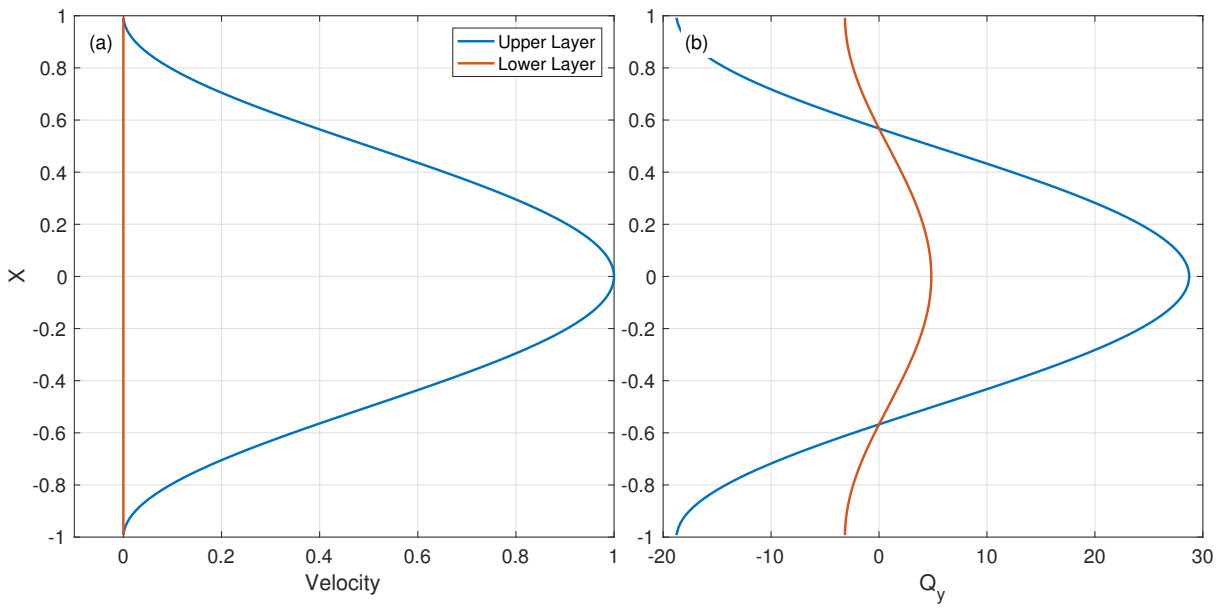

Figure 6: An example velocity profile and PV gradient for $\beta = 1$, $F = 4$ for cosine jet case.

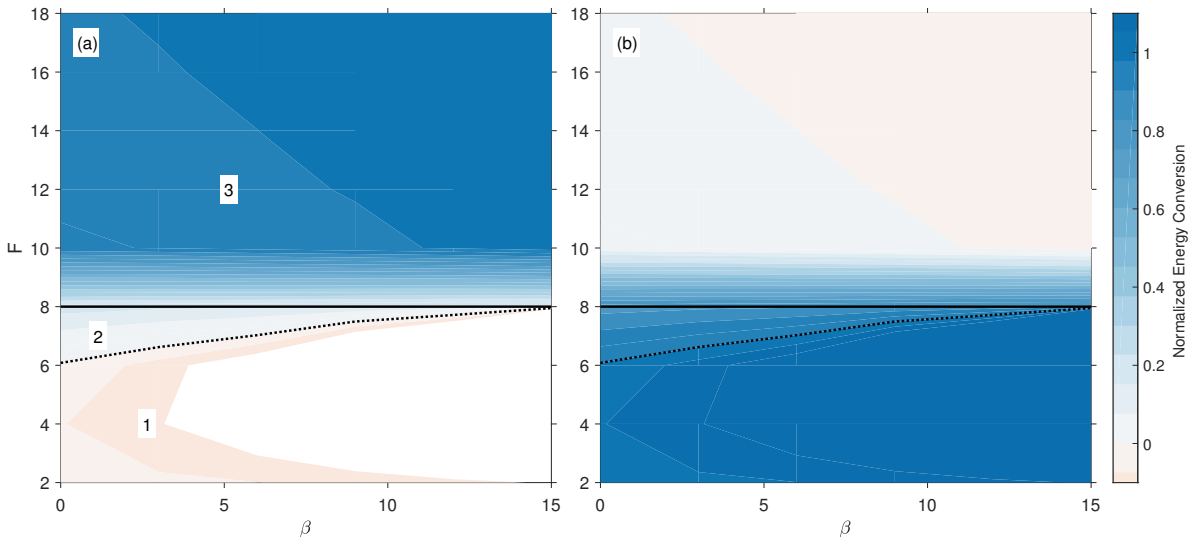

Figure 7: Energy conversion computed for the most unstable eigenfunctions normalized by total (potential plus kinetic) energy conversion for cosine jet. Potential energy conversion (a) and kinetic energy conversion (b). The dotted line shows where the momentum fluxes change sign and the solid line shows where the PV gradient changes sign between layers, with no sign below and a sign change above. Blue represents downgradient fluxes and red represents up-gradient fluxes.

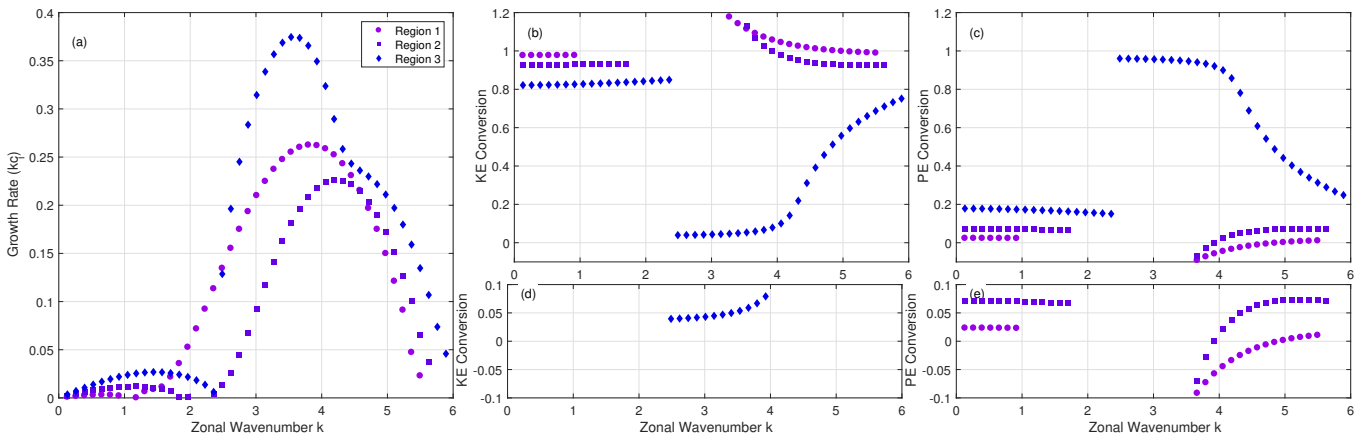

Figure 8: Example growth rates and normalized energy conversions from 3 different regions. Growth rates (a), kinetic energy conversion (b,d) and potential energy conversion (c,e). See text for locations. Region 1: $F = 4$, $\beta = 1$. Region 2: $F = 7$, $\beta = 1$. Region 3: $F = 10$, $\beta = 1$.